Electronic Supplementary Material (ESI) for Soft Matter.

Shear jamming and fragility in fractal suspensions under confinement

Sarika C. K.,[1] Sayantan Majumdar,[1] and A. K. Sood[2]

[1]*Soft Condensed Matter Group, Raman Research Institute, Bengaluru 560080, India*

[2]*Department of Physics, Indian Institute of Science, Bengaluru 560012, India*

(Dated: November 3, 2022)

FRACTAL STRUCTURE OF MWCNT FLOCS

For the fractal structure analysis, MWCNT suspension ($\phi = 0.03\%$) is drop cast onto a glass substrate and dried. Optical microscopic images of the drop cast samples show the fractal nature of MWCNT flocs. The 2D fractal dimension (d_f) is estimated by two methods: Area-Perimeter analysis ($log(A) \propto d_f\ log(P)$) and box-counting method ($d_f = -\lim_{r\to 0} \frac{log(n)}{log(r)}$ where n is the number of filled boxes and r is the box size). The Area-Perimeter analysis using the image of discrete flocs (Fig. S1a) yields the value $d_f = 1.64$ (see Fig. S1b). For the box-counting method, images of interconnected flocs are collected in which the fractal arrangement of nanotubes is clear. A typical image and the fractal dimension estimation ($d_f = 1.53$) are shown in Fig. S1c and d respectively. As we increase the concentration for drop casting, such analysis becomes difficult due to the dense packing of the dried clusters. So, we have used a very dilute sample ($\phi = 0.03\%$) for such analysis.

The concentration of the drop cast sample is low compared to that of the sample used for rheology measurements. At those higher concentrations, it becomes difficult to image the fractal arrangement of nanotubes due to clustering. To address this issue, we have directly estimated the 3D fractal dimension of the suspension used for the rheology measurement from the effective volume fraction: $\phi_{eff} \approx \phi(R/a)^{3-d_f}$, where R is the radius of gyration and a is the size of MWCNT [1]. Using the image of dispersed broken flocs in the flowing state (Fig. S4c), the estimated value of 3D fractal dimension is, $d_f \approx 2.1$ ($\phi_{eff} = 36.3\%$, $\phi = 0.77\%$, $R = 100\mu$m and $a = 1\mu$m). Here, we have considered only the flowing state of the sample just beyond yielding, where the isolated clusters are observed that enables us to estimate the value of R. In the CJ and SJ states, the determination of R is difficult using optical imaging due to the connectivity of the clusters. For the estimation of effective volume fraction, the area coverage of the dispersed broken flocs (Fig. S4c) is measured using ImageJ software. Assuming a uniform distribution of flocs across the shear gap, ϕ_{eff} is estimated.

FLOW CURVES OF MWCNT SUSPENSIONS

Flow curves of MWCNT suspensions of different volume fractions ranging from 0.26% to 5.35% are plotted as viscosity versus applied shear stress in Fig. S2. Shear jamming

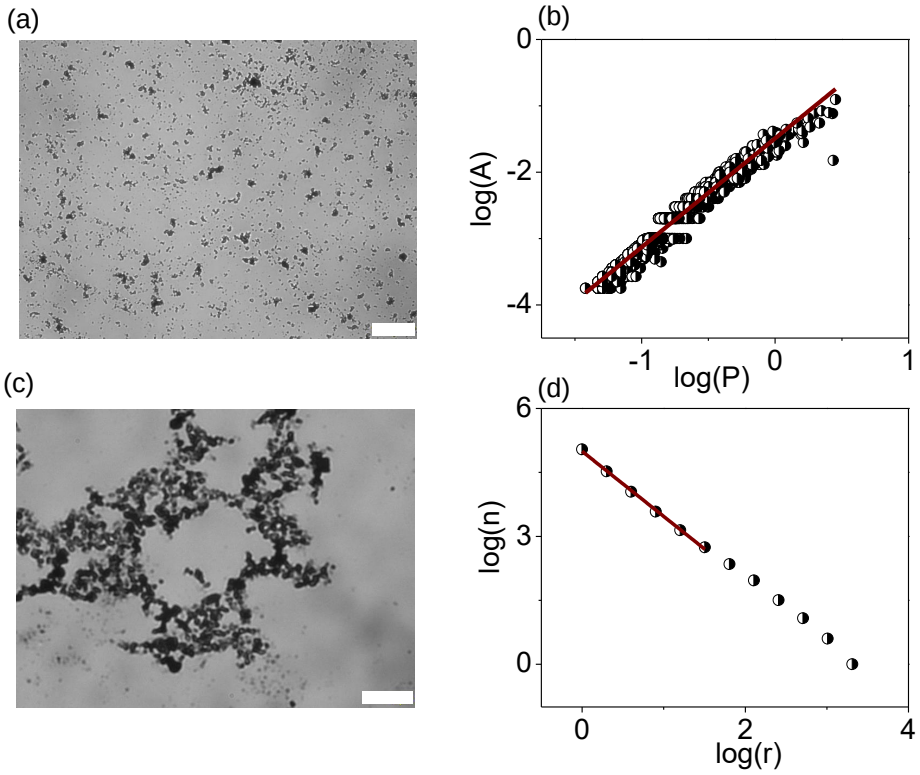

FIG. S1. a) Optical image of discrete MWCNT fractal flocs (scale bar: 50 μm). b) Log(A) versus log(P) of the individual flocs and the linear fit. c) Optical image of the interconnected fractal flocs (Scale bar: 20 μm). d) Log(n) versus log(r) of the interconnected flocs and the linear fit.

transition is observed for $\phi \geq 0.5\%$. From the variation of viscosity with shear stress, $\eta \sim \tau^{\delta}$, the onset of DST is characterized with, $\delta = 1$. Here, the divergence of viscosity at finite shear stress and the corresponding drop in shear rate, $\dot{\gamma} \sim 0$, imply direct manifestation of shear jamming without prior DST.

Since MWCNT suspensions belong to the category of frictional suspensions which exhibit DST or SJ or both, we use S-shaped flow curve representation [2] of the rheological data in Fig. S3a. In the S-shaped flow curve, SJ is indicated by arch-shapes with a vanishing $\dot{\gamma}$ at higher stress. A magnified portion of the flow curve ($\phi = 2.5\%$) is shown in Fig. S3b. It clearly shows that the shear rate drops down to the resolution limit of the rheometer and fluctuates around zero in regions I and III. Since the average shear rate is negligible in these regions, they are solid-like jammed states; namely, cohesive jammed state and shear jammed state.

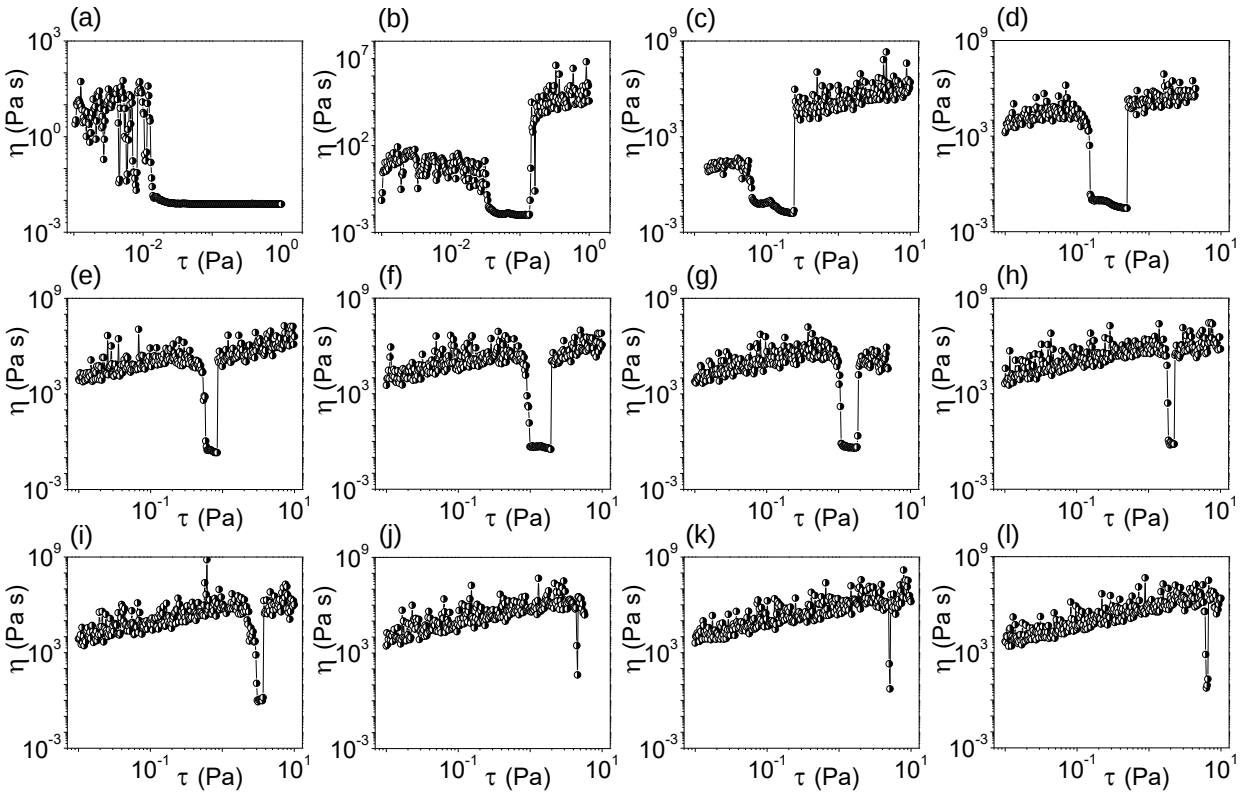

FIG. S2. a - l) Flow curves of MWCNT suspensions of different volume fractions, 0.26, 0.51, 1.02, 1.52, 2.01, 2.51, 2.99, 3.47, 3.95, 4.42, 4.89, 5.35% respectively, plotted as viscosity versus shear stress in log-log scale.

STRESS REVERSAL IMAGES

In situ optical images of MWCNT suspension ($\phi = 0.77\%$) collected in transmission mode during the stress reversal with a wide-angle lens (Leica, 5x) are shown in Fig. S4. It shows the structural transformations associated with the initial flow of suspensions when shear stress of 3 Pa is applied. The structural deformation pathways leading to the shear jamming can be clearly seen in the images.

PARAMETERS FOR THE MODELING

For modeling the rheology data of MWCNT suspensions using the combined constitutive model of Herschel-Bulkley and Wyart-Cates, we used parameter values, $n = 0.2$, $k = 0.1$ and $\eta_0 = 1.65$ mPa s. The critical volume fraction of jamming without friction, $\phi_0 = 5.4\%$,

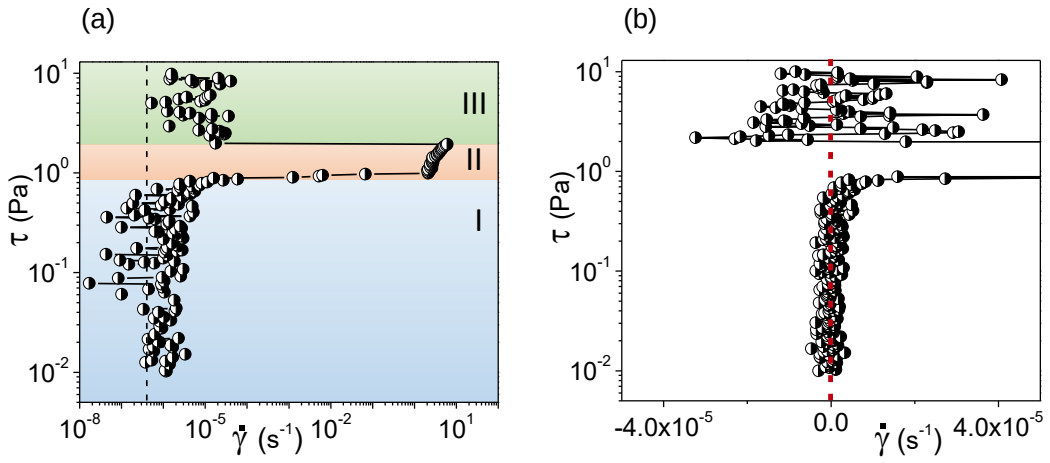

FIG. S3. a) S-shaped flow curve of MWCNT suspension ($\phi = 2.5\%$), plotted as shear stress versus shear rate in log-log scale. The dashed line denotes the shear rate at the resolution limit of the rheometer. b) Magnified portion of the flow curve showing the fluctuation of shear rate around zero (vertical dashed line) in both CJ and SJ states.

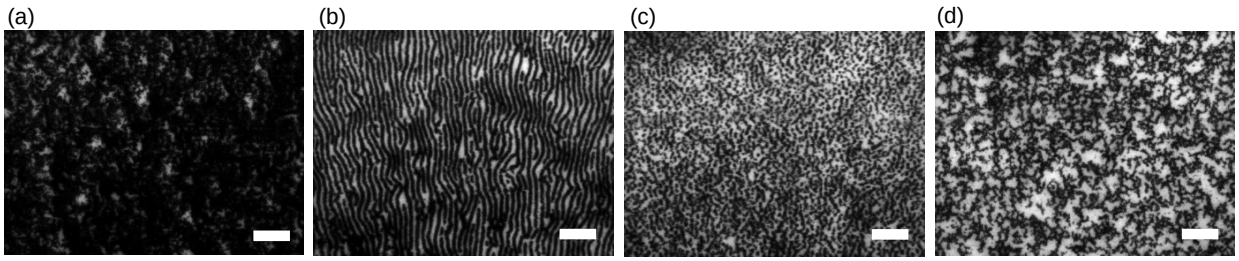

FIG. S4. Optical images taken after the application of shear stress (3 Pa). It shows diffuse MWCNT network structure at the quiescent state (a), rolling log-like flocs (b) and dispersed broken flocs (c) at the flowing-state and interconnected dense floc network structure at the SJ state (d). Scale bar: 1 mm.

is the volume fraction above which the system remains in the CJ state under the application of shear stress. The critical volume fraction of jamming with friction, $\phi_\mu = 0.51\%$, is the volume fraction above which the system exhibits shear jamming.

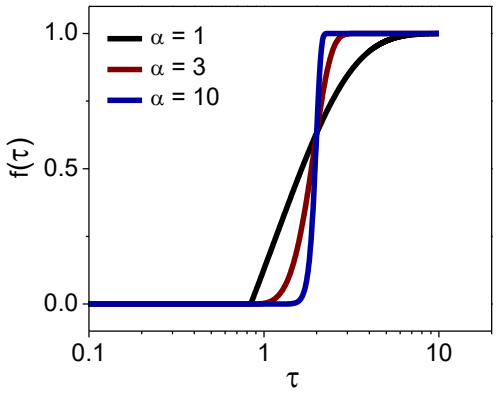

FIG. S5. Growth of $f(\tau)$ with shear stress for different growth rates, $\alpha = 1$, 3 and 10.

$f(\tau)$ GROWTH AT DIFFERENT RATES

Growth of fraction of frictional contacts with shear stress, $f(\tau) = 1 - e^{-(\frac{\tau-\tau_y}{\tau^*-\tau_y})^\alpha}$ for $\tau > \tau_y$ and $f(\tau) = 0$ for $\tau \leq \tau_y$, for different values of growth rates, $\alpha = 1$, 3 and 10, is shown in Fig. S5.

[1] D. B. Genovese, Advances in Colloid and Interface Science, 2012, 171–172, 1–16.

[2] M. Wyart and M. Cates, Physical review letters, 2014, 112, 098302.